METHODS

Grain Boundary Imaging and Orientation Analysis

Backscatter electron (BSE) maps of thin sections were acquired using the FEI Verios XHR scanning electron microscope (SEM) at the Centre for Microscopy and Analysis (CMCA) at The University of Western Australia, Perth. Analytical conditions are listed in Table 1.

The two different grain boundary assemblages were colour coded on each of the thin section BSE maps. The assemblage shape and orientation (Fig. 3 A) was analysed using the Analyze Particles tool in ImageJ (Schneider et al., 2012). Orientation data was then plotted using Stereonet 10 (Cardozo and Allmendinger, 2013) and shape data was plotted and fitted with Gaussian curves using the Curve Fitting Toolbox in MATLAB.

Mineral Chemistry and Calculation of Assemblage Composition

The average modal composition of grain boundary assemblages was calculated through combined electron backscatter diffraction (EBSD) and energy dispersive X-ray spectroscopy (EDS) using the MIRA variable pressure field-emission scanning electron microscope (VP-FE-SEM) at the John de Laeter Centre, Curtin University, Perth. Analytical conditions are listed in Table 1.

Modal compositions of grain boundary assemblages were then combined with mineral compositions acquired by wavelength-dispersive X-ray spectroscopy (WDS) on the JEOL 8530F electron probe micro analyser (EMPA) at the CMCA. Analytical conditions are listed in table 1.

The precursor plagioclase composition used in the isocon chemical diagram (Fig. 4 A) was calculated through quantitative WDS mapping of the core of a large (> 1mm diameter) plagioclase grain in the least altered anorthosite, using the operating conditions listed in Table 1.

Table DR1 – Analytical conditions for instruments used.

Instrument	Verios XHR SEM	MIRA VP-FESEM	JEOL 8530F EMPA
Analysis type	BSE imaging	EDS and EBSD	WDS
Working distance	4 mm	20 mm	13 mm
Acceleration voltage	15 keV	20 keV	15 keV
Beam intensity		17 nA	
Beam current	0.8 nA	5 nA	15 nA

Bulk Rock Composition and Thermodynamic Modelling

The bulk rock concentrations of major element oxides in samples have been determined by X-Ray Fluorescence (XRF) spectrometry. The obtained compositions of the anorthosite and amphibolite samples are consistent with those calculated based on modal abundance (TIMA) and phase composition (EPMA) and are thus considered representative (for comparison see Table DR1).

Thermodynamic modelling was undertaken using the software THERMOCALC 3.45 (Powell and Holland, 1988) and the internally consistent thermodynamic dataset and equation of state for H_2O of Holland and Powell (2011). The NCKFMASHTO (Na_2O-CaO -K_2O-FeO-MgO-Al_2O_3-SiO_2-H_2O-TiO_2-Fe_2O_3) system was used with the solution models given in Table 2.

Table DR2– Mineral solution models used for the computation of P-T pseudosections in THERMOCALC 3.45

Solution model	used abbreviation	References
Clinopyroxene	dio	Green et al. (2016)
Clinoamphibole	hb	Green et al. (2016)
Epidote	cz	Holland and Powell (2011)
Garnet	g	White et al. (2014)
Orthopyroxene	opx	White et al. (2014)
Muscovite	mu	White et al. (2014)
Biotite	bi	White et al. (2014)
Ternary feldspar	pl	Holland and Powell (2003)
Tonalitic 'metabasite' melt	L	Green et al. (2016)

REFERENCES CITED

Cardozo, N., Allmendinger, R.W., 2013. Spherical projections with OSXStereonet. Computers & Geosciences 51, 193-205.

Green, E., White, R., Diener, J., Powell, R., Holland, T., Palin, R., 2016. Activity–composition relations for the calculation of partial melting equilibria in metabasic rocks. Journal of Metamorphic Geology 34, 845-869.

Holland, T., Powell, R., 2003. Activity–composition relations for phases in petrological calculations: an asymmetric multicomponent formulation. Contr. Mineral. and Petrol. 145, 492-501.

Holland, T., Powell, R., 2011. An improved and extended internally consistent thermodynamic dataset for phases of petrological interest, involving a new equation of state for solids. Journal of Metamorphic Geology 29, 333-383.

Powell, R., Holland, T., 1988. An internally consistent dataset with uncertainties and correlations: 3. Applications to geobarometry, worked examples and a computer program. Journal of metamorphic Geology 6, 173-204.

Schneider, C.A., Rasband, W.S., Eliceiri, K.W., 2012. NIH Image to ImageJ: 25 years of image analysis. Nature methods 9, 671.

White, R., Powell, R., Holland, T., Johnson, T., Green, E., 2014. New mineral activity–composition relations for thermodynamic calculations in metapelitic systems. Journal of Metamorphic Geology 32, 261-286.

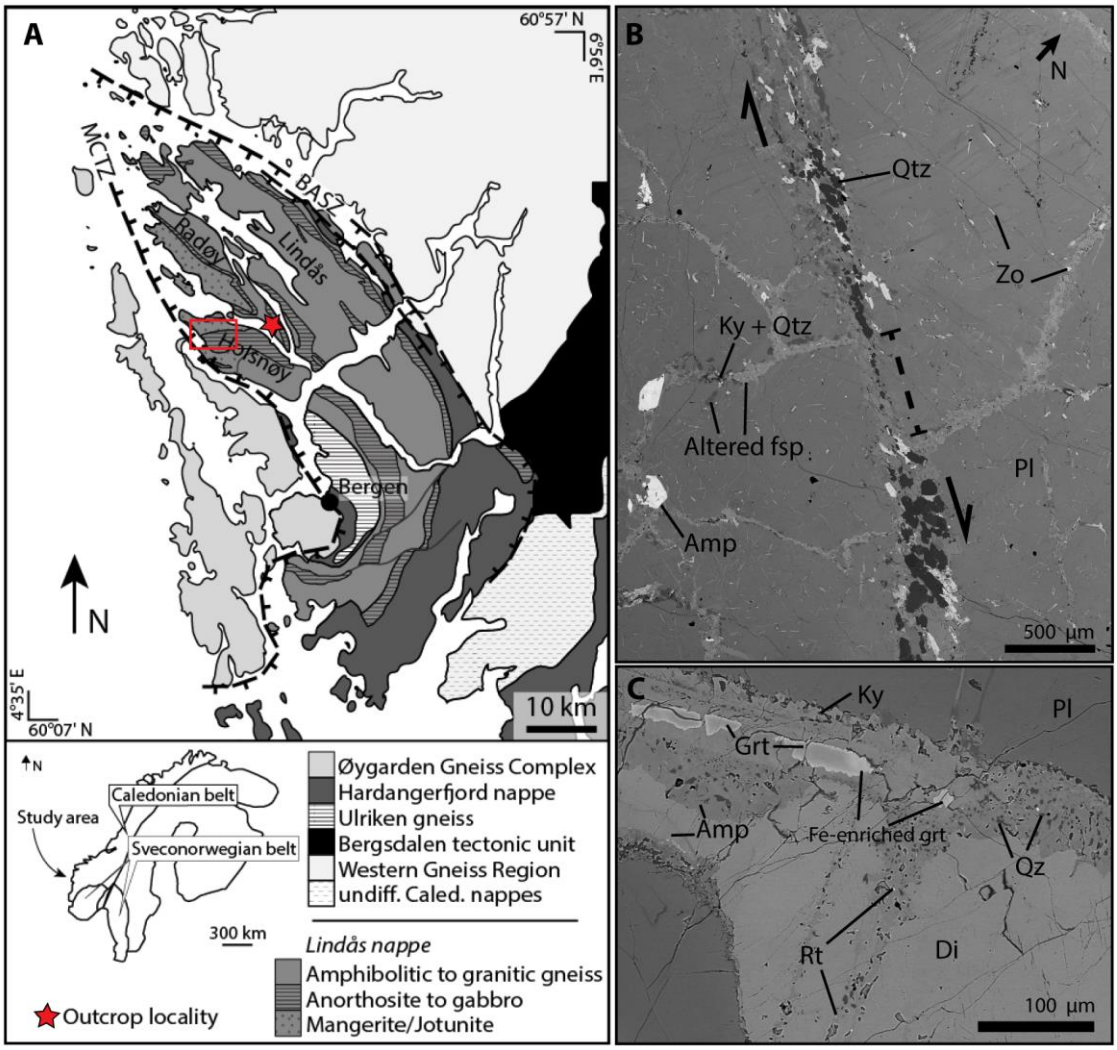

Figure DR1 – Study locality and details of alteration (A) Sample location (red star) at Radøy in the Lindås Nappe of the Bergen Arc, Western Norway. Sample location in Universal Transverse Mercator [UTM] coordinates relative to World Geodetic System 1984 [WGS84]; zone 31V, 620260E, 6718524N. The red box indicates the location of eclogite shear zones studied by Raimbourg et al. (2005). MCTZ = Main Caledonian Thrust Zone. BASZ = Bergen Arc Shear Zone. Modified from Boundy et al. (1997) and Glodny et al. (2008) (B) Backscatter electron (BSE) image showing the offset of an original plagioclase grain boundary (indicated by dashed line) along an extensional quartz-vein, indicating a dextral top-to-the-ESE sense of displacement during hydration of the anorthosite. (C) BSE image of the alteration assemblage occurring at diopside and garnet grain boundaries, primarily consisting of hornblende with minor quartz, rutile and Fe-enriched garnet.

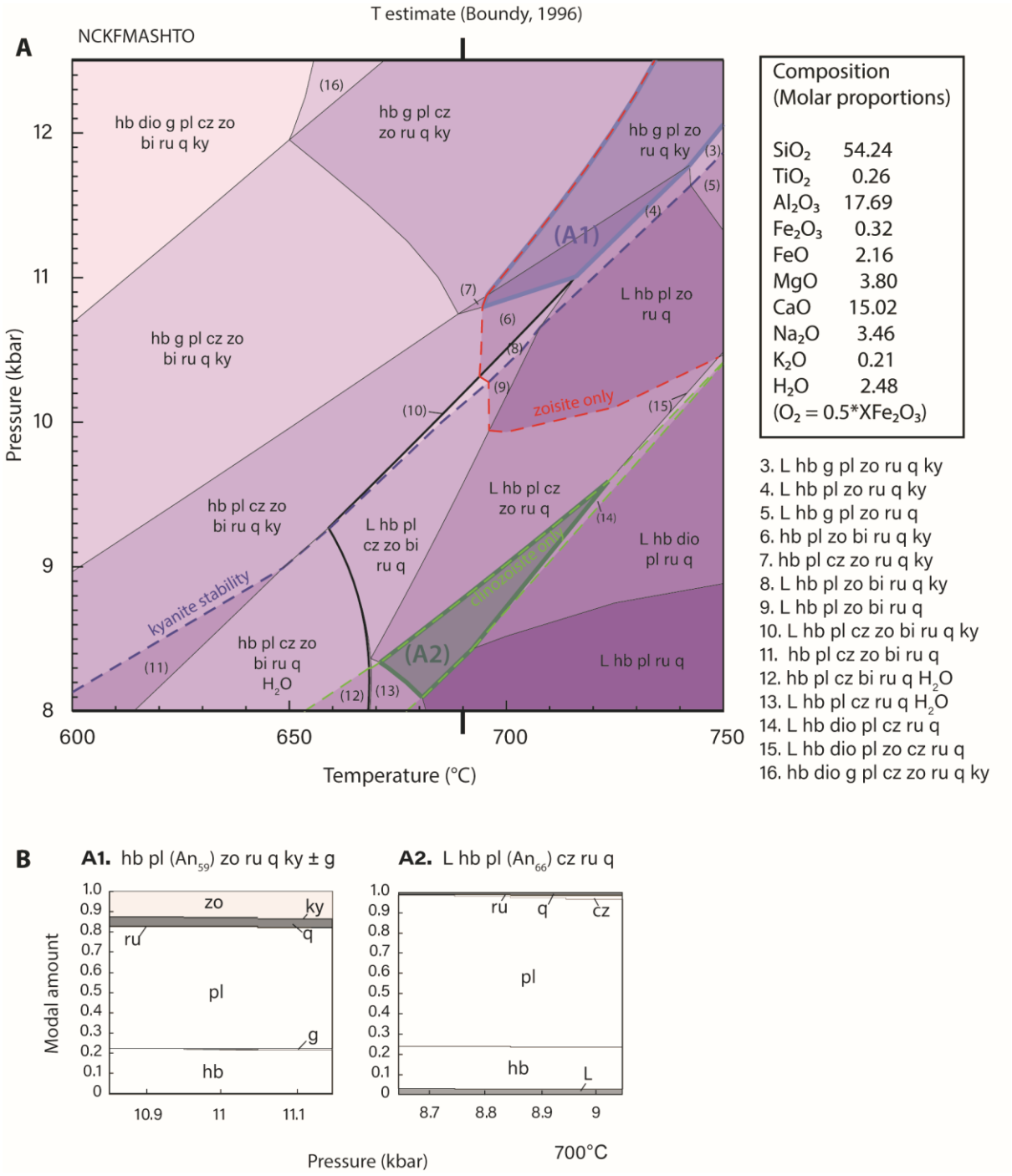

Figure DR3 – Thermodynamic modelling of amphibolite bulk rock (A) Pseudosection for amphibolite assemblages. The PT space of the two grain boundary assemblages is outlined in bold lines and coloured according to the scheme used in the manuscript. (B) Modelled modal compositions for assemblages at 700°C are given for each of the assemblages. The An-component estimates produced by THERMOCALC are consistent with the observed plagioclase compositions. An_{58} for A1, consistent with the composition of the host plagioclase and An_{66} for A2.

Table DR3 – Bulk XRF (used in isocon diagram Fig. 4 A) and TIMA map calculated whole rock composition for granulitic anorthosite and amphibolite, and, local composition of grain boundary assemblages I and II, calculated using modal mineral volumes and electron microprobe mineral compositions (All values are weight% oxide; sample density is in g/cm^3; n.m. = not measured; LOI = loss on ignition)

Analytical technique	XRF*	TIMA-X	XRF*	TIMA-X	EBSD + WDS	EBSD +WDS	Quantitative WDS mapping*
	Granulitic anorthosite		Amphibolite		Assemblage I	Assemblage II	Precursor plagioclase
Sample density	2.87		2.86				
SiO_2	49.9	50.5	48.9	49.9	57.8	52.8	53.7
TiO_2	0.11	0.12	0.21	0.32	0.02	0.02	0.20
Al_2O_3	27.0	26.5	26.5	27.6	30.8	28.3	29.3
Fe_2O_3	3.58	0.60	3.50	0.81	0.71	0.14	0.19
FeO	n.m.	2.28	n.m.	2.37	0.01	0.23	n.m.
MgO	3.68	3.33	4.11	3.08	0.03	0.44	0.03
CaO	11.9	12.6	11.8	12.9	9.46	11.4	11.9
Na_2O	3.24	3.55	3.23	3.28	0.00	3.49	4.71
K_2O	0.27	0.27	0.28	0.30	0.35	2.33	0.28
LOI	0.22	n.m.	0.83	n.m.	n.m.	n.m.	n.m.
H_2O	n.m.	0.01	n.m.	0.68	0.83	0.12	n.m.
Total	99.8	99.8	100	99.8	100	99.3	100

* All Fe calculated as Fe_2O_3